Synthesis, Crystal Structure, and Magnetic Properties of $[Ni(N_3)_2(2,2\text{-dimethylpropane-}1,3\text{-diamine})]_n$, an Infinite Bidimensional Antiferromagnetic Polymer Presenting Weak 3-D Ferromagnetism

Joan Ribas,*,† Montserrat Monfort,† Xavier Solans,‡ and Marc Drillon§

Departament de Química Inorgànica, Universitat de Barcelona, Diagonal, 647, 08028-Barcelona, Spain, Departament de Cristal.lografia i Mineralogia, Universitat de Barcelona, Martí Franqués, s/n 08028-Barcelona, Spain, and Groupe des Matériaux Inorganiques, EHICS, 1, rue Blaise Pascal, 67008-Strasbourg, France

Received August 4, 1993®

The reaction between aqueous solutions of $Ni(ClO_4)_2$, NaN_3 and 2,2-dimethylpropane-1,3-diamine (Me_2tn) gives blue-green crystals of the title compound which presents N_3^- in a new coordination mode. The new complex $(C_5H_{14}N_8Ni)_n$ crystallizes in the monoclinic system, space group $P2_1/c$, with $a = 12.649(3)$ Å, $b = 7.031(2)$ Å, $c = 12.114(3)$ Å, $\beta = 112.39(2)°$, $V = 996.1(8)$ Å^3, $Z = 4$, $R = 0.059$, and $R_w = 0.059$. The Ni(II) atoms are octahedrally coordinated by two nitrogen atoms of the amine ligand, one N_3^- terminal ligand and three other bridging N_3^- ligands shared by three Ni(II) atoms, giving the stoichiometry $[Ni(N_3)(N_3)_{3/3}(Me_2tn)]$. Each bridging azido ligand coordinates two Ni(II) ions in end-on mode but, at the same time, this azido ligand coordinates the neighboring Ni(II) in an end-to-end mode. This new and unexpected coordination mode of the azido ligand stabilizes a bidimensional polymer made of μ-(1,1-N_3)$_2$Ni$_2$ units linked together by the bridging azides, thus creating a kind of metallomacrocycle which repeats throughout the layer. Magnetic measurements from room temperature down to 60 K show a typical 2D antiferromagnetic behavior; at around 60 K an abrupt field-dependent peak of susceptibility is observed, indicating a long-range magnetic ordering with a net magnetic moment (canting). Magnetization curves at low temperature clearly confirm the presence of weak ferromagnetism. The canted spin structure is analyzed in view of the structure and the single-ion anisotropy of the Ni(II) ion.

Introduction

The azido group is a versatile bridging ligand which can coordinate two Ni(II) ions in either end-to-end[1-4] or end-on fashion.[5-9] Complexes of both kinds have been characterized structurally and magnetically. Dinuclear compounds were first investigated,[1-8] but very recently tetranuclear[9] and even 1D (uniform[10] and altenating[11]) systems have been reported by the authors. Magnetostructural correlations have explained the different behaviors[4,12] (ferromagnetic or antiferromagnetic) according to the coordination of the azide to Ni(II), and the results have been compared to those for the well-documented analogous Cu(II).[13-15] In all cases, 1,3-coordination promotes antiferromagnetic behavior while 1,1-coordination entails ferromagnetism. Systematic studies with bidentate amines have enabled us to isolate new Ni(II) complexes with unexpected magnetic behavior. Thus, a preliminary study of $[Ni(N_3)_2(2,2\text{-dimethylpropane-}1,3\text{-diamine})]_n$ has shown that this complex exhibits an unusual structure with two kinds of coordination mode (1,1 and 1,3) for nickel(II) ions and bidimensional magnetic behavior.[16] Very recently Tuchagues et al. have emphasized that 2D antiferromagnetic compounds with highly anisotropic ions, such as iron(II), are good candidates for stabilizing canted spin structures and, accordingly, molecular ferromagnets.[17] Thus, a net magnetic moment was reported in Fe(4-imidazoleacetate)$_2$ for $T_c < 15$ K.[17] In this paper we discuss the structure and magnetic properties of $[Ni(N_3)_2(2,2\text{-dimethyl-}1,3\text{-propanediamine})]_n$, which constitutes a new molecular ferromagnet with a remarkable ordering temperature.

Experimental Section

Materials. 2,2-Dimethylpropane-1,3-diamine (Me_2tn) (Aldrich), nickel perchlorate (Fluka), and sodium azide (Fluka) were purchased and used without further purification.

Synthesis. *Caution!* Metal complexes with azide and organic ligands are potentially explosive. Only a small amount of materials should be prepared, and the material should be handled with caution.

† Departament de Química Inorganica, Universitat de Barcelona.
‡ Departament de Cristallografia i Mineralogia, Universitat de Barcelona.
§ EHICS.
® Abstract published in *Advance ACS Abstracts,* January 15, 1994.

(1) Wagner, F.; Mocella, M. T.; D'Aniello, M. J.; Wang, A. H. J.; Barefield, E. K. *J. Am. Chem. Soc.* **1974**, *96*, 2625.
(2) Pierpont, C. G.; Hendrickson, D. N.; Duggan, D. M.; Wagner, F.; Barefield, E. K. *Inorg.Chem.* **1975**, *14*, 604.
(3) Chaudhuri, P.; Guttman, M.; Ventur, D.; Wieghardt, K.; Nuber, B.; Weiss, J. *J. Chem. Soc., Chem. Commun.* **1985**, 1678.
(4) Ribas, J.; Monfort, M.; Diaz, C.; Bastos, C.; Solans, X. *Inorg. Chem.* **1993**, *32*, 3557.
(5) Arriortua, M. I.; Cortes, A. R.; Lezama, L.; Rojo, T.; Solans, X.; Font-Bardia, M. *Inorg. Chim. Acta.* **1990**, *174*, 263.
(6) Escuer, A.; Vicente, R.; Ribas, J. *J. Magn. Magn. Mater.* **1992**, *110*, 181.
(7) Vicente, R.; Escuer, A.; Ribas, J.; El-Fallah, M. S.; Solans, X.; Font-Bardía, M. *Inorg. Chem.* **1993**, *32*, 1920.
(8) Ribas, J.; Monfort, M.; Diaz, C.; Bastos, C.; Solans, X. *Inorg. Chem.* in press.
(9) Ribas, J,: Monfort, M.; Costa, R.; Solans, X. *Inorg. Chem.* **1993**, *32*, 695.
(10) Escuer, A.; Vicente, R.; Ribas, J.; Salah el Fallah, M.; Solans, X. *Inorg. Chem.* **1993**, *32*, 1033.
(11) Vicente, R.; Escuer A.; Ribas, J.; Solans, X. *Inorg. Chem.* **1992**, *31*, 1726.
(12) Escuer, A.; Vicente, R.; Ribas, J.; El Fallah, M. S.; Solans X.; Font-Bardía, M. *Inorg. Chem.* **1993**, *32*, 3727.
(13) Charlot, M. F.; Kahn, O.; Chaillet, M.; Larrieu, C. *J. Am. Chem. Soc.* **1986**, *108*, 2574.
(14) (a) Kahn, O.; Sikorav, S.; Gouteron, J.; Jeannin, S.; Jeannin, Y. *Inorg. Chem.* **1983**, *22*, 2877. (b) Sikorav, S.; Bkouche-Waksman, I.; Kahn, O. *Inorg. Chem.* **1984**, *23*, 490.
(15) Commarmond, J.; Plumere, P.; Lehn, J. M.; Agnus, Y.; Louis, R.; Weiss, R.; Kahn, O.; Morgersten-Badarau, I. *J. Am. Chem. Soc.* **1982**, *104*, 6330.
(16) Monfort, M.; Ribas, J.; Solans, X. *J. Chem. Soc. Chem. Commun.* **1993**, 350.
(17) Martínez-Lorente M. A., Tuchagues, J. P.; Pétrouléas, V.; Savariault, J. M.; Poinsot, R.; Drillon, M. *Inorg. Chem.* **1991**, *30*, 3587.

0020-1669/94/1333-0742$04.50/0

Table 1. Crystallographic Data for $[Ni(N_3)_2(Me_2tn)]_n$

chem formula: $C_5H_{14}N_8Ni$	fw = 244.93
a = 12.649(3) Å	space group; $P2_1/c$
b = 7.031(2) Å	T = room temp
c = 12.114(3) Å	λ = 0.710 69 Å
β = 112.39(2)°	ρ_{calcd} = 1.633 g cm^{-3}
V = 996.1(8) Å^3	μ = 19.21 cm^{-1}
Z = 4	R^a = 0.059
	$R_w{}^b$ = 0.059

^{a} $R = \Sigma||F_o| - |F_c||/\Sigma|F_o|$. ^{b} $R_w = \Sigma w||F_o| - |F_c||/\Sigma w|F_o|$.

Table 2. Final Atomic Coordinates (×10^4, Ni × 10^5) of $C_5H_{14}N_8Ni$

	x/a	y/b	z/c	B_{eq},^{a} Å^2
Ni	5673(5)	15177(9)	43349(5)	1.58(3)
N(1)	459(4)	1120(7)	6071(4)	1.99(19)
N(2)	458(3)	2246(7)	6794(3)	1.67(19)
N(3)	460(5)	1631(7)	2490(4)	2.66(22)
N(4)	−958(4)	2982(7)	3808(4)	2.35(21)
N(5)	−1676(4)	2642(7)	2854(4)	2.34(21)
N(6)	−2388(5)	2260(11)	1936(5)	4.50(31)
N(7)	1996(4)	−178(7)	4893(5)	2.14(20)
N(11)	1503(5)	3986(7)	4736(5)	2.32(21)
C(8)	3077(5)	493(9)	5087(6)	2.69(26)
C(9)	3464(5)	2446(9)	5537(5)	2.48(24)
C(10)	2676(6)	3989(9)	5669(7)	2.74(26)
C(12)	4631(6)	2837(15)	6532(9)	4.83(13)
C(13)	3540(7)	2456(13)	4313(8)	3.86(37)

^{a} $B_{eq} = (8\pi^2/3)U_{ij}a_i^*a_j^*a_ia_j$.

By addition of a solution of 0.65 g (2 mmol) of NaN_3 to an aqueous solution containing 1.89 g (1 mmol) of $Ni(ClO_4)_2{\cdot}6H_2O$ and 0.51 g (1 mmol) of 2,2-dimethylpropane-1,3-diamine (Me_2tn), a green microcrystal powder of $[Ni(Me_2tn)(\mu\text{-}N_3)_2]_n$, previously reported by us,[8] immediately precipitates. The mother liquor was left undisturbed, and blue-green crystals of the title compound were obtained after several days by slow evaporation. With the stoichiometric amount of $Ni(SO_4){\cdot}H_2O$ instead of $Ni(ClO_4)_2$ the same complex was obtained in low yield.

Spectral and Magnetic Measurements. IR spectra were recorded on a Nicolet 520 FTIR spectrophotometer. Magnetic measurements were carried out on polycrystalline samples (40 mg) with a pendulum type magnetosusceptometer (MANICS DSM-8) equipped with a **TBT** Helium continuous flow cryostat, working in the range 4.2–300 K and a Drusch EAF 16UE electromagnet. The magnetic field was approximately 1.5 T. Diamagnetic correction was evaluated as 125 × 10^{-6} cm^3 mol^{-1} from Pascal's tables.

X-ray Crystallography. A prismatic crystal (0.1 × 0.1 × 0.2 mm) was selected and mounted on a Philips PW-1100 diffractometer. Unit cell parameters were determined from automatic centering of 25 reflections ($8° < \theta < 12°$) and refined by the least-squares method. Intensities were collected with graphite monochromatized MoK_α radiation using the ω scan technique. A total of 1533 reflections were measured in the range $2° \le \theta \le 25°$, 1352 of which were assumed as observed applying the condition $I \ge 2.5\sigma(I)$. Three reflections were measured every 2 h as orientation and intensity control; significant intensity decay was not observed. Lorentz-polarization and absorption corrections were made. The crystallographic data, conditions used for the intensity data collection, and some features of the structure refinement are listed in Table 1. The structure was solved by Patterson synthesis, using the SHELXS computer program,[18] and refined by full-matrix least-squares methods, with the SHELX76 computer program.[19] The function minimized was $\Sigma w||F_o| - |F_c||^2$, where $w = (\sigma^2(F_o) + 0.0057|F_o|^2)^{-1}$. f, f′ and f″ were taken from ref 20. The positions of all H atoms were located from a difference synthesis and refined with an overall isotropic temperature factor. The final R factor was 0.059 (R_w = 0.059) for all reflections observed. Number of refined parameters was 170. Maximum shift/esd = 0.1, and the maximum and minimum peaks in final difference synthesis were +0.4 and −0.4 e Å^3 respectively. Final atomic coordinates are given in Table 2.

(18) Sheldrick, G. M. *Acta Crystallogr.* **1990**, *A46*, 467.
(19) Sheldrick, G. M. SHELX: A computer program for crystal structure determination. University of Cambridge, England, 1986.
(20) *International Tables for X-Ray Crystallography;* Kynoch Press: Birmingham, England, 1974.

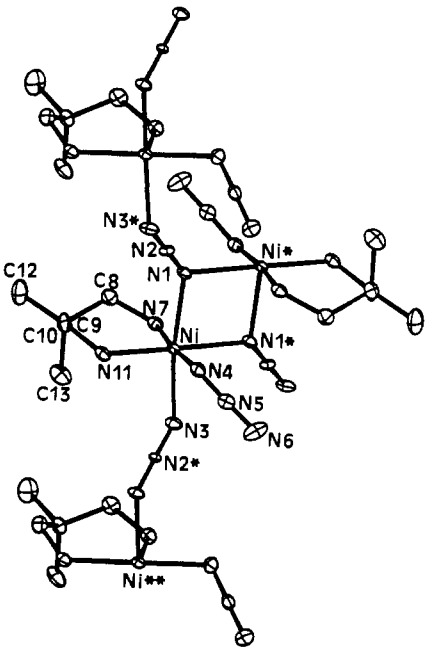

Figure 1. Atom-labeling scheme for $[Ni(N_3)_2(2,2\text{-dimethylpropane-}1,3\text{-diamine})]_n$.

Table 3. Main Bond Distances (Å) and Angles (deg) for $C_5H_{14}N_8Ni$

N(1)–Ni	2.177(4)	Ni–Ni	3.312(1)
N(1)^i–Ni	2.209(4)	N(2)–N(1)	1.118(6)
N(3)–Ni	2.188(5)	N(2)–N(3)^{iii}	1.154(6)
N(4)–Ni	2.062(5)	N(5)–N(4)	1.191(7)
N(7)–Ni	2.053(5)	N(6)–N(5)	1.165(7)
N(11)–Ni	2.052(5)		
N(3)–Ni–N(1)	171.5(2)	N(1)^i–Ni–N(3)	90.0(2)
N(4)–Ni–N(1)	88.1(2)	N(1)^i–Ni–N(4)	87.1(2)
N(4)–Ni–N(3)	88.8(2)	N(1)^i–Ni–N(7)	87.4(2)
N(7)–Ni–N(1)	88.8(2)	N(1)^i–Ni–N(11)	178.7(2)
N(7)–Ni–N(3)	93.5(2)	N(2)–N(1)–Ni	130.4(4)
N(7)–Ni–N(4)	174.0(2)	Ni–N(1)–Ni^{ii}	98.1(4)
N(11)–Ni–N(1)	97.1(2)	Ni^{ii}–N(1)–N(2)	124.2(4)
N(11)–Ni–N(3)	91.0(2)	N(1)–N(2)–N(3)^i	179.0(4)
N(11)–Ni–N(4)	92.2(2)	Ni^{iii}–N(3)–N(2)^{ii}	138.8(4)
N(11)–Ni–N(7)	93.3(2)	N(5)–N(4)–Ni	118.5(4)
N(1)^i–Ni–N(1)	81.9(2)	N(6)–N(5)–N(4)	177.8(6)

Results

IR and Analytical Data. The most characteristic bands are those attributable to the azido ligand: the ν_{as} at 2050 (vs) and 2080 cm^{-1} (vs) agree with the two kinds of azido ligands (terminal and bridging). The other two bands of the N_3^- group (ν_s and δ) are masked by the amine bands. One important feature in the IR spectrum is the presence of five sharp medium bands in the amine region (1200, 1150, 1100, 1060, and 985 cm^{-1}). The elemental analyses (C, N, H, Ni) for different syntheses are consistent with the formulation. Anal. Calcd/found for $C_5H_{14}N_8Ni$: C, 24.52/24.3; H, 5.76/5.7; N, 45.75/45.8; Ni, 23.97/24.0.

Crystal Structure. The structure consists of neutral sheets linked in the crystal lattice by van der Waals forces. In these sheets, each Ni(II) is octahedrally coordinated by two nitrogen atoms of the Me_2tn ligand, one N_3^- terminal ligand, and three other bridging N_3^- shared by three Ni(II), giving a total stoichiometry of $[Ni(N_3)(N_3)_{3/3}(Me_2tn)]$. The structure of one Ni(II) with its surroundings is shown in Figure 1. The bond lengths and angles are gathered in Table 3. From Figure 1 and Table 3, we may point out the distortion of the Ni(II) environment: Ni–N(1) and Ni–N(3) distances are similar, 2.177 and 2.188 Å; Ni–N(7) and Ni–N(4) are also similar, 2.053 and 2.062 Å, respectively, but significantly shorter than the above distances. Finally, the two other distances, Ni–N(11) and Ni–N(1*), are

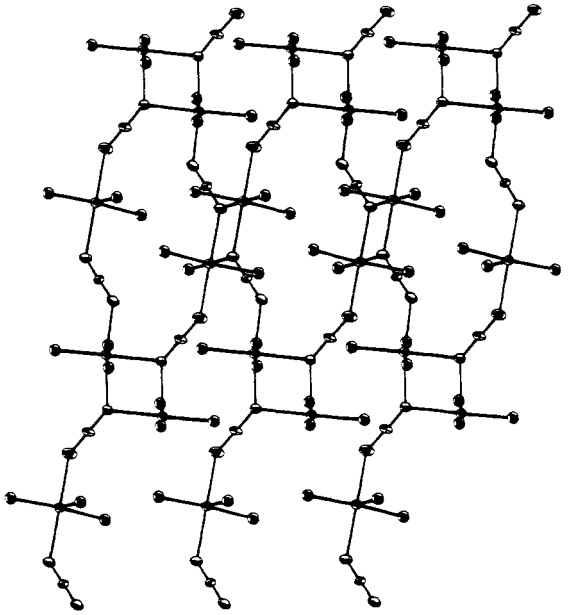

Figure 2. Perpendicular view of one layer for $[Ni(N_3)_2(2,2\text{-dimethylpropane-1,3-diamine})]_n$.

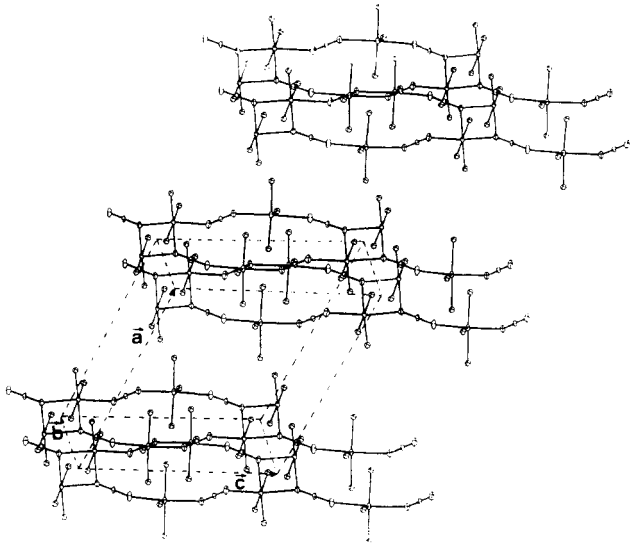

Figure 3. Crystal structure, showing three layers for $[Ni(N_3)_2(2,2\text{-dimethylpropane-1,3-diamine})]_n$.

markedly different, 2.052 and 2.209 Å, respectively. These distances, together with the corresponding angles (Table 3) induce a great distortion in the Ni(II) site. This distortion is an important feature for the analysis of magnetic measurements. On the other hand, each Ni(II) is bonded to another Ni(II) by two azido bridging ligands in 1,1 (end-on) mode, giving an asymmetrical planar entity [Ni–N(1)–Ni*–N(1*)] (Figure 1). The two Ni(II) ions are related by an inversion center. This feature has already been found in several dinuclear Ni(II) complexes in which the two Ni(II) cations are linked by two N_3^- in end-on mode.[5-8] This dinuclear entity is coordinated to four dinuclear entities and so on, giving a neutral layer. This kind of coordination is shown in Figure 2. As can be seen from Figures 1 and 2, this new coordination mode between dinuclear entities is achieved through an azido bridging ligand in 1,3 (end-to-end) coordination mode. From structural and magnetic points of view it is important to point out that the angle between two of these correlated μ-(1,1-$N_3)_2Ni_2$ dinuclear entities (assumed to be completely planar) is 57.10°. Figure 2 shows a schematic representation of one layer formed between these entities. In Figure 3 some of these layers have been represented in order to clarify the whole structure. The

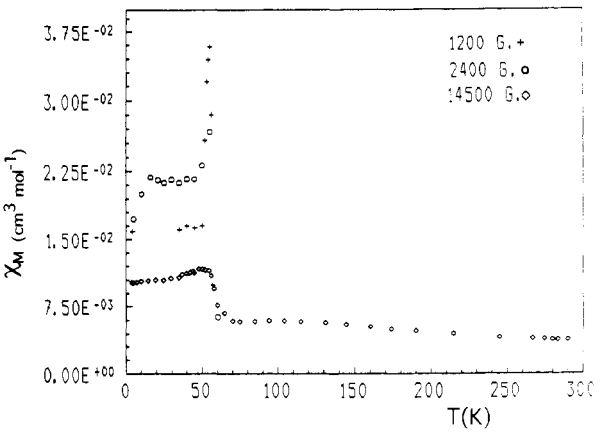

Figure 4. Experimental temperature dependence of χ_M at different fields for $[Ni(N_3)_2(2,2\text{-dimethylpropane-1,3-diamine})]_n$.

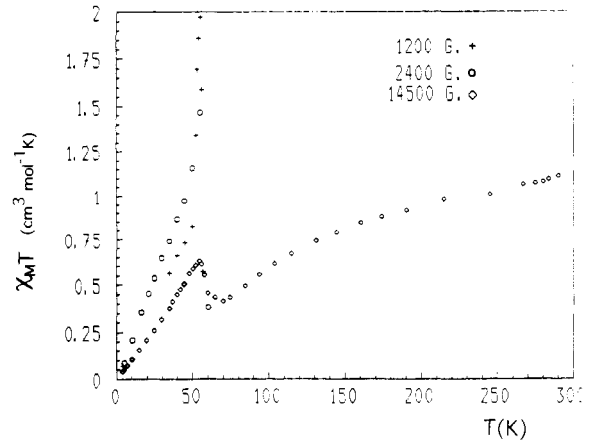

Figure 5. Experimental temperature dependence of $\chi_M T$ at different fields for $[Ni(N_3)_2(2,2\text{-dimethylpropane-1,3-diamine})]_n$.

shortest distance between these layers occurs in C(8)–C(12) = 3.895 Å, H(8)–H(12) = 2.81 Å, H(8)–H(12B) = 3.08 Å, and H(8A)–H(12A) = 2.58 Å.

Magnetic Results. The magnetic behavior of the new 2-D complex is shown in Figures 4 and 5 as plots of the χ_M and $\chi_M T$ product vs temperature (K). From room temperature down to approximately 60 K these figures exhibit a behavior typical of planar Heisenberg magnets very similar to that of isotropic antiferromagnetic chains, because the two systems have in common the absence of long range order. Then a decrease in the $\chi_M T$ vs T curve and a broad maximum in the χ_M vs T curve (90–100 K) is observed due to short-range order effects. There is no theory available for fitting these results.[21] Further cooling causes abrupt and field-dependent change in the χ_M and $\chi_M T$ curves: a strong increase in the susceptibility values is observed when the field is lowered, indicating a transition to a long-range magnetic ordering (T_c = 55 K). Below T_c, a plateau in the susceptibility values is observed. Such behavior is typical of the 1-D or 2-D antiferromagnetic systems showing a weak ferromagnetism at low temperature (canted systems).[21] Magnetization measurements at 4.2 K are shown in Figure 6. When the magnetic field is cycled between +18 and −18 kG, a characteristic hysteresis loop is obtained with a remanent magnetization of $6 \times 10^{-3} \mu_b$ and a coercive field of 2800 Oe (Figure 6). These results show that the saturation of the magnetization occurs at a value that is far from the theoretical value for an $S = 1$ spin system ($2\mu_b$); the net magnetic moment at zero field agrees with a canted spin system.

Magnetostructural Correlations. Close examination of the X-ray molecular and crystal structure suggests an explanation

(21) Carlin, R. L. *Magnetochemistry*; Springer-Verlag: Berlin, 1986; pp 206–212.

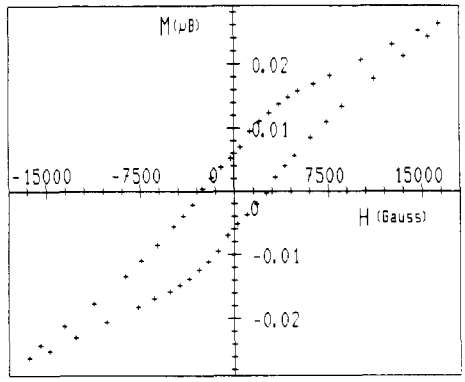

Figure 6. Hysteresis loop ($M/N\beta$ vs H) at 4.2 K for $[Ni(N_3)_2(2,2\text{-dimethylpropane-1,3-diamine})]_n$.

for the origin of the weak ferromagnetism observed. According to Carlin,[21] two principle mechanisms explain the canted systems: antisymmetric exchange and/or single-ion anisotropy. The first , the antisymmetric part of the spin-exchange Hamiltonian $H = \mathbf{d}_{ij}\cdot[S_i \times S_j]$[22-24] cants the spins S_i and S_j because the coupling energy is minimized when the spins are perpendicular to each other. $\mathbf{d}$ is proportional to $[(g-2)/g]J$. For octahedral Ni(II) systems in which g values are close to 2.00, the canting is more likely to be due to the second cause: the single-ion anisotropy, as in NiF_2, a typical case described by Moriya.[25] In this rutile-like structure, the antisymmetric exchange is zero by symmetry requirements, but Ni(II) suffers a distortion which results in marked zero-field splitting. Moriya[25] reported that the canted structure results not from the axial distortion (which must be positive) but from competition between the exchange parameter J (which tends to align the spins parallel or antiparallel) and the rhombic zero-field splitting term, $\mathbf{E}$, which causes the perpendicularity of the spins of different lattice sites. Consequently, there is a compromise in which the spins are tilted away from the parallelism. Some canted examples with Mn(III) or Fe(II) have been reported in recent years: one-dimensional systems of Mn(III)[26-28] and one bidimensional Fe(II) system.[17] Mn(III) complexes, which a strong Jahn–Teller distortion, provide evidence for the hypothesis that single ion anisotropy is the cause of canted behavior. For our purpose it is important to remark that symmetry restrictions apply equally to both mechanisms: in particular, ions with magnetic moments in a unit cell cannot be related by a center of symmetry if canting occurs. These remarks may lead to a move accurate interpretation of the canting behavior of the title complex. In $[Ni(N_3)_2(Me_2tn)]_n$, the closest Ni(II) ions, namely Ni–Ni*, linked by two N_3^- bridges in 1,1 mode are related by an inversion center. Similar 1,1-N_3^- bridging ligand complexes isolated elsewhere are shown to be ferromagnetically coupled.[5-9] According to the structure, these dinuclear units are linked through N_3^- bridges in end-to-end mode, known to promote antiferromagnetic coupling.[1-4,10-12] It is to be noted that, unlike the previous unit, there is no inversion center between Ni* and Ni** (Figure 1). Further, the antiferromagnetic coupling through end-to-end N_3^- bridges is usually stronger than the ferromagnetic coupling within μ-(1,1-N_3)$_2$Ni$_2$ units. As a result, it can be expected that (i) distinct spin sublattices occur between adjacent μ-(1,1-N_3)$_2$-Ni$_2$ pairs and (ii) due to the site symmetries (the μ-(1,1-N_3)$_2$Ni$_2$ units are tilted by 57.1°) the anisotropy axes are different from one pair to the next.

Owing to the competition between antiferromagnetic coupling through N_3^- ligands and zero field splitting effects with different axes from one pair to the other, the situation is very similar to that reported by Tuchagues et al.[17] for a 2-D canted Fe(II) complex. Clearly, such a canted structure can only occur below the 3-D transition temperature (T_c), even if the origin is related to the symmetry and exchange couplings within Ni(II) layers.

Finally, it should be emphasized that the interactions between these magnetic layers are likely to be of van der Waals type, promoting the three dimensional ordering observed. The long-range ordering temperature is among the highest reported so far, but it should be noted that the net magnetic moment remains weak with regard to the Fe(II) complex.

Acknowledgment. This work was undertaken with the financial support of CICYT Grant PB90/0029.

Supplementary Material Available: Tables giving crystal data and details of the structure determination, atom coordinates, bond lengths, bond angles, anisotropic thermal parameters, and hydrogen atom parameters (6 pages). Ordering information is given on any current masthead page.

(22) Dzyaloshinsky, I. *J. Phys. Chem. Solids* **1958**, *4*, 241.
(23) Silvera,I. F.; Thorneley, J. H. M.; Tinkman, M. *Phys. Rev.* **1964**, *136*, A695.
(24) Keffer, F. *Phys. Rev.* **1962**, *126*, 896.
(25) Moriya, T. *Phys. Rev.* **1960**, *117*, 635.
(26) Gregson, A. K.; Moxon, N. T. *Inorg. Chem.* **1982**, *21*, 586.
(27) Kennedy, B. J.; Murray, K. S. *Inorg. Chem.* **1985**, *24*, 1552.
(28) Kirk, M. L.; Soo Lah, M.; Raptopoulou, C.; Kessissoglou, D. P.; Hatfield, W. E.; Pecoraro, V. L. *Inorg. Chem.* **1991**, *30*, 3900.